

Engineering entanglement between resonators by hot environment

M. Tahir Naseem¹ and Özgür E. Müstecaplıoğlu^{1,2,*}

¹*Department of Physics, Koç University, 34450 Sariyer, Istanbul, Türkiye*

²*TÜBİTAK Research Institute for Fundamental Sciences, 41470 Gebze, Türkiye*

Autonomous quantum thermal machines do not require an external coherent drive or work input to perform the desired tasks, making them a promising candidate for thermal management in quantum systems. Here, we propose an autonomous quantum thermal machine in which two uncoupled macroscopic mechanical resonators or microwave resonators achieve considerable entanglement via a hot thermal bath. This becomes possible by coupling the resonators to a common two-level system or third harmonic oscillator and driving it by the hot incoherent thermal bath. The critical step to make the entanglement involves suitable engineering of the hot bath, realized by bath spectrum filtering. Our results suggest that the bath spectrum filtering can be an alternative to typical non-autonomous reservoir engineering schemes to create exotic quantum states.

I. INTRODUCTION

Entanglement plays a key role in the quantum information processing and quantum technologies [1]. Therefore, the generation and protection of entanglement in quantum systems is of paramount importance. However, due to the unavoidable coupling of the quantum systems with their environments, entanglement generally degrades or lost. To counter the decoherence caused by system-environment coupling, several schemes have been proposed that exploit the non-unitary evolution of quantum systems to create steady-state entanglement [2–5]. The so-called “reservoir engineering” scheme has been proposed in several physical systems [2–13] and experimentally realized in atomic systems [14–17]. The idea of reservoir engineering is extended to optomechanical systems for the generation of entanglement between optical or mechanical resonators [18–21]. In reservoir engineering, desired dissipative dynamics is obtained by engineering effective reservoirs using external classical controls or work inputs.

In a different approach, entanglement can be created at thermal equilibrium by coupling a composite quantum system to a cold bath, and sufficient cooling the system may lead to an entangled state [22, 23]. In the absence of thermal equilibrium, the temperature gradient can be used to create entanglement [24–43]. These works show that the energy current between the reservoirs generates entanglement between the quantum systems [34–37, 39, 40]. More specifically, a recent study shows that a critical value of heat flow is required for the emergence of entanglement between two coupled qubits [39]. However, in all these proposals, additional filtering operation or feedback is required to make the amount of entanglement significantly large [35, 39], with the exception of a coupled qubits system [44]. Alternatively, a hot reservoir with effective negative temperature can be employed for entanglement enhancement [36]. These entanglement generation proposals are for composite two-level systems with some exceptions of works based on optical and atomic oscillators [25, 45], and d -dimensional composite systems [46]. Here, we propose creating entanglement between non-interacting macroscopic mechanical resonators via an effective common hot bath. The

higher temperature of the hot bath can create significantly large entanglement without the use of additional feedback or filtering operations.

In this work, we ask these questions: Is it possible to devise a scheme in which dissipative dynamics can be engineered for transient or steady-state entanglement in an autonomous setting? If yes, is it possible to create significant entanglement between uncoupled macroscopic mechanical resonators without the need for additional feedback? We answer these questions in the affirmative by employing simple spectral filtering of the thermal baths present in the system. Hence incorporating the advantages of reservoir engineering in autonomous entanglement generation thermal machines. For the implementation of our scheme, we consider two uncoupled mechanical or microwave resonators interacting with a common ancilla system via *energy-field* coupling [47–49]. By employing simple reservoir engineering based on spectral filtering of the thermal baths, mechanical resonators dissipatively evolve to an entangled steady-state. Note that spectral filtering to engineer reservoirs differs from typical reservoir engineering schemes [6], and local filtering operations which are used to enhance entanglement in the out-of-equilibrium systems [46]. In a typical reservoir engineering scheme, external control or work input is required to obtain desired effective dissipation of the system. Contrary, bath spectrum filtering do not require time-dependent interactions or external classical control, making our entanglement machine truly ‘quantum.’ Bath spectrum filtering was pioneered by G. Kurizki and co-workers [50] and applied to enhance several thermal tasks such as output power [51], efficiency at maximum power [52], thermal management [53], simultaneous cooling of resonators [54], and antibunching of a phonon field [55].

Compared with previous proposals of autonomous thermal entanglement machines, our scheme has several distinct advantages: (i) We use simple filtering of the thermal baths to engineer an effective reservoir that governs the resonators’ dissipative dynamics. It is well-known that the two-mode squeezing interaction with sufficiently low temperature is sufficient in a typical entanglement generation scheme, such as in multimode optomechanical systems [21]. However, our proposal differs entirely from previously reported optomechanics schemes [18, 19, 21], which rely on external control drives to obtain effective two-mode squeezing interac-

* omustecap@ku.edu.tr

tion between the uncoupled resonators. On the contrary, we employ only incoherent thermal baths to induce two-mode squeezing-like environment-mediated interactions between the resonators. (ii) The amount of entanglement increases monotonically with the temperature gradient, allowing entanglement between the resonators in the presence of a hot environment. In the previous proposals, there exists an optimal value of temperature gradient for maximum entanglement, after which entanglement starts decreasing [25, 35]. We note that in some fermionic systems, entanglement increases monotonically with the temperature gradient [44]. (iii) Our machine can create significant entanglement between uncoupled macroscopic mechanical resonators without the need for additional feedback or filtering operation [35]. (iv) Cooling and entanglement generation between the resonators occur simultaneously in our scheme (see appendix A for details).

The rest of the paper is organized as follows. In Sec. II we describe the model system for the implementation of our scheme. Then in Sec. III derivation of the master equation is given for the system analysis. The results for the entanglement quantification is discussed in Sec. IV. Finally, we present conclusions of this work in Sec. V.

II. MODEL SYSTEM

In our scheme, we consider a model shown in Fig. 1. It consists of a two-level system or a harmonic oscillator interacting with the two resonators R_1 and R_2 via *longitudinal* (optomechanical-like) coupling [48]. The Hamiltonian of this system is given by [49, 56–59] (we take Plank's constant $\hbar = 1$)

$$\hat{H}_S = \omega_a \hat{n}_a + \sum_{i=1,2} \omega_i \hat{b}_i^\dagger \hat{b}_i + \sum_{i=1,2} g_i \hat{n}_a (\hat{b}_i + \hat{b}_i^\dagger), \quad (1)$$

with ω_a (ω_i) being the frequency of the subsystem A (R_i), and g_i is the interaction strength between A and resonators R_i . The annihilation (creation) operator of the resonator R_i is denoted by \hat{b}_i (\hat{b}_i^\dagger). $\hat{n}_a = \hat{a}^\dagger \hat{a}$ is the number operator of the resonator A , with \hat{a}_i and \hat{a}_i^\dagger being annihilation and creation operators, respectively. In case of a TLS, \hat{n}_a is replaced by Pauli spin matrix $\hat{\sigma}_z$ and ω_a is multiplied by a factor of 1/2 in Eq. (1).

Note that the Hamiltonian given in Eq. (1) can be realized in various setups. For example, the TLS can be an electronic spin qubit [63], a superconducting qubit [61, 62], a quantum dot [60], or lower two levels of an optical resonator under weak excitation approximation [65]. The subsystem A can also be an optical or microwave resonator [48, 49, 59]. Further, R_i can be nanomechanical resonators [48], or superconducting transmission line resonators [49, 59]. Hence our scheme is not limited to a specific setup. In our numerical results, we use the parameters representative of an electromechanical system [64].

In addition to interaction with resonators, subsystem A is coupled with two thermal baths of temperatures T_h and T_c . Each resonator R_i is unavoidably coupled to its environment

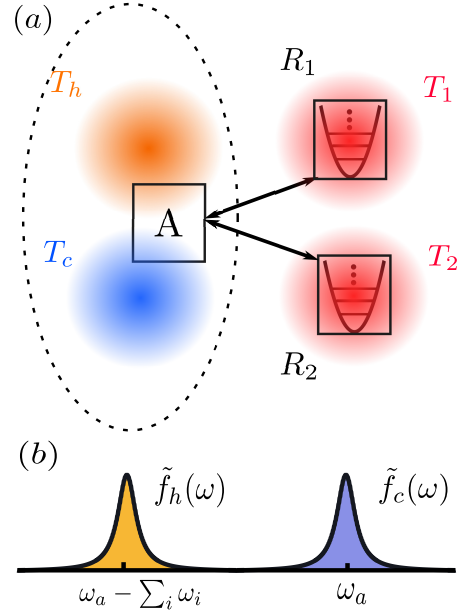


FIG. 1. (a) Model description. Our autonomous entanglement generation thermal machine consists of a two-level system (TLS) or a harmonic oscillator A simultaneously coupled with two harmonic oscillators R_i via *energy-field* interaction [48, 49]. Subsystem A can be a quantum dot [60], a superconducting qubit [61, 62], an electronic spin [63], an optical or microwave resonator [48]. The harmonic oscillators R_i can be microwave [59] or nanomechanical resonators [64]. The resonators R_i are unavoidably coupled to their thermal environments of temperature T_i , and subsystem A is coupled to two thermal baths of temperatures T_h and T_c . All these thermal baths are independent and can have any non-negative temperature in the limit $T_h > T_i > T_c$. The black dashed oval shows that taking a trace over subsystem A gives an effective joint bath for R_i , which may creates quantum correlations between the resonators R_i . (b) Spectrally filtered baths spectra. $\tilde{f}_h(\omega)$ and $\tilde{f}_c(\omega)$ are the filtered spectra of the hot and cold baths, respectively. The width and center of the filtered bath spectrum can be controlled by the system-bath interaction strength and filter frequency [see Eq. (18)]. The subsystem A and resonators R_i frequencies are given by ω_a and ω_i , respectively. These spectrally separated filtered baths lead to a dissipative dynamics given in Eq. (20).

modeled by an ensemble of oscillators with a thermal distribution of temperature T_i . The need to couple A with two thermal baths is because we shall simultaneously cool the resonators R_i to their ground-state before the entanglement generation step. The cooling requires a hot bath which helps to remove energy from resonators and dump it into a cold bath [52, 54]. Moreover, our scheme involves bath spectrum filtering to obtain non-overlapping baths spectra [Fig. 1(b)], in which each bath can only induce transitions of a single frequency. In this case, the energy transfer is only possible if A is coupled with at least two baths [52, 54, 55, 66]. We assume all the baths can attain any non-negative finite temperature provided $T_h > T_i > T_c$. The free Hamiltonian of the thermal baths is given by

$$\hat{H}_E = \sum_{k,E} \omega_{k,E} \hat{c}_{k,E}^\dagger \hat{c}_{k,E}, \quad (2)$$

with $E = h, c, i$, and $\omega_{k,E}$ being the frequency of k th mode and $\hat{c}_{k,E}$ ($\hat{c}_{k,E}^\dagger$) is corresponding bosonic annihilation (creation) operator. The sum is taken over the infinite number of bath modes indexed by k . The interaction of the isolated $A - R_i$ system with the environments is given by

$$\hat{H}_{S-E} = \sum_{k,q=h,c} g_{k,q}(\hat{a} + \hat{a}^\dagger)(\hat{c}_{k,q} + \hat{c}_{k,q}^\dagger) + \sum_{k,i} g_{k,i}(\hat{b}_i + \hat{b}_i^\dagger)(\hat{c}_{k,i} + \hat{c}_{k,i}^\dagger), \quad (3)$$

with $g_{k,q}$ ($g_{k,i}$) being the coupling strength between the A (resonators R_i) with the k th mode of the bath. In case of a TLS, operators \hat{a} and \hat{a}^\dagger are replaced by respective $\hat{\sigma}_-$ and $\hat{\sigma}_+$ matrices.

III. THE MASTER EQUATION

The microscopic derivation of the master equation requires first to diagonalize the Hamiltonian in Eq. (1) using the transformation [67–69]

$$\hat{u} = e^{-\hat{n}_a \sum_i \alpha_i (\hat{b}_i^\dagger - \hat{b}_i)}, \quad (4)$$

where $\alpha_i = g_i/\omega_i$. The diagonalized Hamiltonian has the form

$$\hat{H}_S = \hat{u} \hat{H}_S \hat{u}^\dagger = \omega_a \hat{n}_a + \sum_i \tilde{b}_i^\dagger \tilde{b}_i - \sum_i \frac{g_i^2}{\alpha_i} \hat{n}_a^2. \quad (5)$$

The transformed operators are given by

$$\tilde{a} = \hat{a} e^{-\sum_i \alpha_i (\hat{b}_i^\dagger - \hat{b}_i)}, \quad (6)$$

$$\tilde{b}_i = \hat{b}_i - \alpha_i \hat{n}_a. \quad (7)$$

The master equation can be derived by first transforming the isolated system operators in Eq. (3) by using Eq. (6); then transforming the system operators in Eq. (5) into the interaction picture, and followed by the standard Born-Markov and Secular approximations. The resulting equation has the form [54, 55, 70]

$$\frac{d\tilde{\rho}}{dt} = \tilde{\mathcal{L}}_q \tilde{\rho} + \sum_i \tilde{\mathcal{L}}_i \tilde{\rho}. \quad (8)$$

Here the Liouville super-operators for the subsystem A and baths of the resonators R_i are denoted by $\tilde{\mathcal{L}}_q$ and $\tilde{\mathcal{L}}_i$, respectively. These are given by

$$\begin{aligned} \tilde{\mathcal{L}}_q \tilde{\rho} = & f_q(\omega_a) \{ D[\tilde{a}] + \alpha^3 \sum_i D[\tilde{a} \tilde{b}_i^\dagger \tilde{b}_i] \} + f_q(-\omega_a) \{ D[\tilde{a}^\dagger] + \sum_i \alpha^3 D[\tilde{a}^\dagger \tilde{b}_i^\dagger \tilde{b}_i] \} + \sum_{i,n=1,2} \alpha^{n+1} \{ f_q(\omega_a - n\omega_i) D[\tilde{a} \tilde{b}_i^{\dagger n}] \\ & + f_q(-\omega_a + n\omega_i) D[\tilde{a}^\dagger \tilde{b}_i^n] + f_q(\omega_a + n\omega_i) D[\tilde{a} \tilde{b}_i^n] + f_q(-\omega_a - n\omega_i) D[\tilde{a}^\dagger \tilde{b}_i^{\dagger n}] \}, + \alpha^3 \left\{ f_q(\omega_a - \sum_i \omega_i) D[\tilde{a} \tilde{b}_1^\dagger \tilde{b}_2^\dagger] \right. \\ & + f_q(-\omega_a + \sum_i \omega_i) D[\tilde{a}^\dagger \tilde{b}_1 \tilde{b}_2] + f_q(\omega_a + \sum_i \omega_i) D[\tilde{a} \tilde{b}_1 \tilde{b}_2] + f_q(-\omega_a - \sum_i \omega_i) D[\tilde{a}^\dagger \tilde{b}_1^\dagger \tilde{b}_2^\dagger] + f_q(\omega_a - \omega_1 + \omega_2) D[\tilde{a} \tilde{b}_1^\dagger \tilde{b}_2] \\ & \left. + f_q(-\omega_a + \omega_1 - \omega_2) D[\tilde{a}^\dagger \tilde{b}_1 \tilde{b}_2^\dagger] + f_q(\omega_a + \omega_1 - \omega_2) D[\tilde{a} \tilde{b}_1 \tilde{b}_2^\dagger] + f_q(-\omega_a - \omega_1 + \omega_2) D[\tilde{a}^\dagger \tilde{b}_1^\dagger \tilde{b}_2] \right\}, \\ \tilde{\mathcal{L}}_i \tilde{\rho} = & f_i(\omega_i) D[\tilde{b}_i] + f_i(-\omega_i) D[\tilde{b}_i^\dagger]. \end{aligned} \quad (9)$$

We note that in the derivation of the master equation, we ignored all higher-order terms $\mathcal{O}(\alpha^4)$ and assumed $\alpha = \alpha_i$ for simplicity. The Lindblad dissipator $D[\hat{\sigma}]$ is defined by

$$D[\hat{\sigma}] = \frac{1}{2} (2\hat{\sigma} \tilde{\rho} \hat{\sigma}^\dagger - \tilde{\rho} \hat{\sigma}^\dagger \hat{\sigma} - \hat{\sigma}^\dagger \hat{\sigma} \tilde{\rho}). \quad (10)$$

The spectral response function of the baths is denoted by $\tilde{f}(\omega)$. In the rest of the paper, unless otherwise mentioned, we consider one-dimensional Ohmic spectral densities for all the thermal baths, given by

$$f_E(\omega) = \begin{cases} \omega \gamma_E [1 + \bar{n}_E(\omega)], & \omega > 0, \\ |\omega| \gamma_E \bar{n}_E(|\omega|), & \omega < 0, \end{cases} \quad (11)$$

and $f_E(0) = 0$ for Ohmic spectral densities of the baths. Here, the system-bath coupling strength is denoted by γ_E , and the mean number of quanta in each thermal bath is given by

(we take the Boltzmann constant $k_B = 1$)

$$\bar{n}_E(\omega) = \frac{1}{e^{\omega/T_E} - 1}. \quad (12)$$

IV. RESULTS AND DISCUSSION

In this section, we shall investigate the entanglement between the resonators in the model presented in Fig. 1. This scheme employs bath spectrum filtering, an instance of reservoir engineering, to generate entanglement between the resonators. For the numerical analysis, we consider the parameters of an electro-mechanical system [57, 64]: $\omega_a = 2\pi \times 10$ GHz, $\omega_i = 2\pi \times 10$ MHz, $\gamma_h = \gamma_c = 2\pi \times 5$ MHz, $\gamma_i = 2\pi \times 100$ Hz, and $g_i = 2\pi \times 500$ KHz, unless otherwise stated.

In the rest of the work, we consider TLS ancilla to illustrate our proposed scheme. If a TLS or a harmonic oscillator interacts with the resonators via *energy-field* coupling [Eq. (1)], an external coherent control drive of frequency $\omega_c = |\omega_a \pm n\omega_i|$ can induce sideband transitions of the order n . For instance, a control drive resonant with the lower first sideband can induce sideband cooling of the resonator [71]. If the drive is resonant with the lower second sideband, it may produce antibunching of the resonator field [72]. In a complementary approach, if an incoherent suitably engineered thermal bath, drives the subsystem A at the lower first sideband, it leads to cooling of resonators, colloquially referred to as “cooling by heating”. In this case, $D[\tilde{a}^\dagger \tilde{b}_i]$ dominates the dissipative dynamics of the system [54]. Similarly, an incoherent drive at the lower second sideband results in the antibunching of the phonon field, in which $D[\tilde{a}^\dagger \tilde{b}_i^2]$ is the dominant source of dissipation [55]. Remarkably, the rate equations derived in both coherent and incoherently driven $A - R_i$ system shares a similar mathematical structure [54, 55].

By noting this analogy, one may consider the incoherent coupling counterpart of the two-mode squeezing interaction, i.e., $D[\tilde{a}^\dagger \tilde{b}_1 \tilde{b}_2]$ ($D[\tilde{a} \tilde{b}_1^\dagger \tilde{b}_2^\dagger]$), may lead to entanglement between the resonators R_i . However, we aim to entangle modes \hat{b}_i and not necessarily the transformed modes \tilde{b}_i . Hence, $D[\tilde{a}^\dagger \tilde{b}_1 \tilde{b}_2]$ in the *local* basis of the resonators, after taking a trace over subsystem A , takes the form

$$D_{\text{ent}} = \text{Tr}_A[\hat{u}^\dagger D[\tilde{a}^\dagger \tilde{b}_1 \tilde{b}_2] \hat{u}] = \langle \hat{n}_a + 1 \rangle D[e^{\hat{c} - \hat{c}^\dagger} (\hat{d} - \hat{c})], \quad (13)$$

with

$$\begin{aligned} \hat{c} &:= \alpha(\hat{b}_1 + \hat{b}_2), \\ \hat{d} &:= \hat{b}_1 \hat{b}_2 + \alpha^2. \end{aligned} \quad (14)$$

In a previous study [10], it was shown that a nonclassical entangled state of two microwave cavity fields could be engineered via a collision model. In this scheme, carefully prepared three-level atoms with coherent external control drives, randomly interact with the cavity fields. This gives an effective dissipative dynamics of the cavity fields, governed by the Liouville super-operator [10]

$$\mathcal{L}_{\text{eff}} \hat{\rho} = \kappa_c D[\hat{c}_-] + \kappa_d D[\hat{d}_-]. \quad (15)$$

Here, $\kappa_{c,d}$ are the dissipation rates and these depend on the specific system parameters. \hat{c}_- and \hat{d}_- are the joint jump operator for the cavity field and given by [10]

$$\begin{aligned} \hat{c}_- &= \frac{1}{\sqrt{2}}(\hat{b}_1 - \hat{b}_2), \\ \hat{d}_- &= \frac{1}{2}\hat{b}_1 \hat{b}_2 - \beta^2, \end{aligned} \quad (16)$$

here β represents the complex amplitude of the coherent states of both cavities. Eq. (15) shows that D_{ent} may lead to an entangled state of the uncoupled resonators R_i . However, there are additional terms in D_{ent} compared with Eq. (15). To see the effect of these terms on entanglement generation, we consider a hypothetical setting where two uncoupled resonators

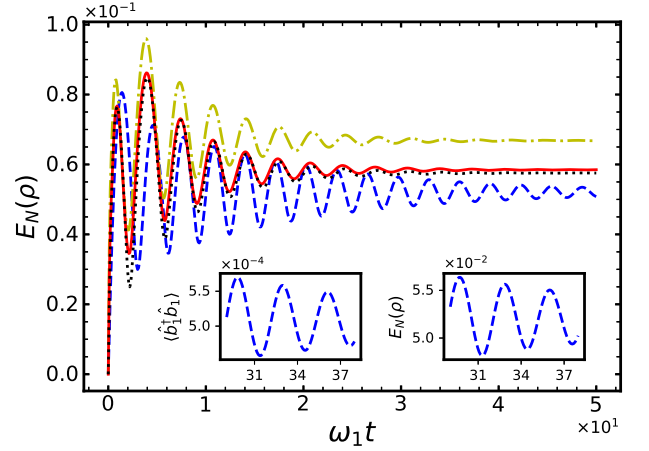


FIG. 2. Physical mechanism of entanglement generation. The logarithmic negativity $E_N(\rho)$ as a function of scaled time $\omega_1 t$. The blue dashed curve is obtained by the numerical integration of Eq. (15), proposed in [10] for generating a two-mode entangled state of optical resonators. The black dotted curve denotes $E_N(\rho)$ for a hypothetical case in which two uncoupled resonators evolve under dissipative dynamics governed by Eq. (13). The yellow dot-dashed and the red solid lines show $E_N(\rho)$ by keeping the first order and second-order terms in α , respectively, and by ignoring all higher-order terms in Eq. (13). The right inset shows a part of the blue dashed curve for $E_N(\rho)$. Finally, in the left inset, the mean number of excitation $\langle \hat{b}_1^\dagger \hat{b}_1 \rangle$ in the resonator R_1 is plotted as a function of scaled time $\omega_1 t$. All these curves show an almost periodic behavior with a period $T \approx 2\pi / \sum_i \omega_i$. Initially, the resonators are prepared in a product of ground-states, $\hat{\rho}(0) = \hat{\rho}_1 \otimes \hat{\rho}_2 = |0_1\rangle \langle 0_1| \otimes |0_2\rangle \langle 0_2|$. In the numerical simulations, we use the Hilbert space with ten photon states for each resonator, and it is verified that the increase in the Hilbert space dimensions does not affect the results. Parameters: $\omega_i = 1$, $\alpha_i = 0.2$, and $\kappa_c = \kappa_d = 0.1$.

evolve under the dissipative dynamics governed by D_{ent} . Per se D_{ent} acts alone, we compare the entanglement results of this setting with that of Eq. (15).

The initial state of the resonators is considered to be a separable ground-state, $\hat{\rho}(0) = \hat{\rho}_1 \otimes \hat{\rho}_2 = |0_1\rangle \langle 0_1| \otimes |0_2\rangle \langle 0_2|$. Other initial states such as thermal state can also be considered; however, entanglement remains small or insignificant for states other than the ground-states of the resonators [10]. To quantify the entanglement between resonators; we use logarithmic negativity [73], which is given by

$$E_N(\hat{\rho}) = \log_2 \|\hat{\rho}^{\Gamma_2}\|. \quad (17)$$

Here, $\hat{\rho}^{\Gamma_2}$ is the partial transpose of the joint density matrix of resonators with respect to R_2 , and $\|\cdot\|$ denotes the trace norm of $\hat{\rho}^{\Gamma_2}$. “In contrast to systems in pure states, bipartite entanglement cannot be uniquely and easily defined in terms of the entropy for systems in mixed states. Among different witnesses and bounds used to examine quantum entanglement in mixed states [74, 75], (logarithmic) negativity is commonly used for characterization of mixed state entanglement in quantum technology and condensed matter applications [75–77]. The main motivations behind its choice are that it is computa-

tionally tractable, it carries a clear operational meaning being an upper bound for distillable entanglement, and it has direct relevance to experimental measurements of mixed state quantum entanglement [78]. Our approach relies on bath induced quantum correlations between subsystems, and hence it is an open quantum system in mixed states, and motivated by these reasons we also choose negativity to quantify quantum entanglement in our case.

The comparison of $E_N(\hat{\rho})$ for two uncoupled oscillators undergoing dissipative dynamics governed by Eq. (13) and Eq. (15) is shown in Fig. 2. All the parameters are considered identical in both cases, including dissipation rates. In the numerical results, we use the Hilbert space size with ten photon states for each resonator and verified that the results do not change by the increase in the Hilbert space size. The result shows that for the considered parameters, entanglement becomes more pronounced in the case of D_{ent} . This result indicates that additional terms in D_{ent} do not destroy the entanglement between the resonators. In the transient regime, both entanglement $E_N(\hat{\rho})$ and populations $\langle \hat{b}_1^\dagger \hat{b}_1 \rangle$ show similar oscillatory behavior with a period $T = 2\pi / \sum_i \omega_i$, and these oscillations vanish in the long time limit. The numerical results in Fig. 2 show that the populations govern the dynamics of the Logarithmic negativity. As $E_N(\hat{\rho})$ is found to be maximum for the maximum values of populations and vice versa. Similar behavior has previously been reported for linearly coupled oscillators evolving under nonlinear dissipation [79].

It is worth mentioning that we do not assume two-mode squeezing-like interaction between the resonators. In our model, the resonators are uncoupled. The microscopic derivation of the master equation (Eq. (9)) results in the bath-mediated incoherent interactions between the resonators, among which two-mode squeezing-like interactions are also present. These incoherent interactions are induced by the thermal environment and should not be mixed with the two-mode squeezing interactions that appear in the system's Hamiltonian. We like to emphasize that it is not the two-mode squeezing-like interactions per se that lead to entanglement between the resonators. The transformation of these dissipators in the “local” basis of the resonators yields required dissipation (Eq. (13)). Hence, only two-mode squeezing-like Lindblad dissipators are not sufficient to create entanglement between the resonators.

It remains to show that, in our scheme, D_{ent} is the dominant source of dissipation in the the dynamics of the system \hat{H}_S given in Eq. (1). To this end, we employ bath spectrum filtering to remove the unwanted dissipative channels. We consider the filtered bath spectra of the hot and cold baths shown in Fig. 1(b) and given by [50–54, 80]

$$\tilde{f}_q(\omega) = \frac{\kappa_q}{\pi} \frac{(\pi f_q(\omega))^2}{(\omega - (\omega_q^r + \Delta_q(\omega))^2 + (\pi f_q(\omega))^2)}. \quad (18)$$

Here κ_q is the coupling strength between subsystem A and the bath filter, and ω_q^r is the resonance frequency of the bath spectrum. The bath induced Lamb shift is given by

$$\Delta_q(\omega) = P \int_0^\infty d\omega' \frac{f_q(\omega')}{\omega - \omega'}, \quad (19)$$

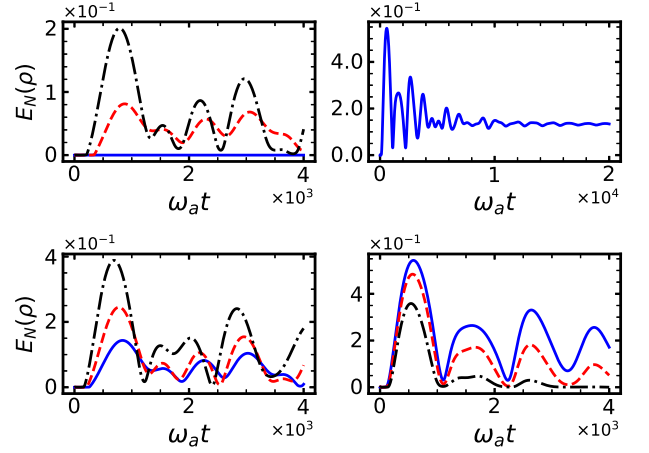


FIG. 3. Entanglement quantification of resonators with different frequencies. Logarithmic negativity $E_N(\rho)$ as a function of scaled time $\omega_a t$. The results are obtained by the numerical integration of Eq. (20) and then using the inverse transformation [Eq. (6)] to get $\hat{\rho}$ in the local basis. Finally, $E_N(\rho)$ is computed numerically using Eq. (17). Initial state of the system is considered a pure separable state of the subsystems, $\hat{\rho}(0) = \hat{\rho}_a \otimes \hat{\rho}_2 = |g_a\rangle \langle g_a| \otimes |0_1\rangle \langle 0_1| \otimes |0_2\rangle \langle 0_2|$, here $|g_a\rangle$ represents the ground state of the TLS. Parameters: $\omega_a = 2\pi \times 10$ GHz, $\omega_1 = 2\omega_2 = 2\pi \times 5$ MHz, $\gamma_h = \gamma_c = 2\pi \times 500$ KHz, $\gamma_i = 2\pi \times 100$ Hz, and $T_c = 65$ mK. All the parameters are scaled with ω_a in the numerical results. (a) Blue solid, red dashed, and black dot-dashed curves are for $T_h = 1, 70, 300$ K, respectively. Here, $T_i = 0.1$ K and $\alpha_i = 0.1$. (b) Long time entanglement $E_N(\rho)$ for $\alpha_i = 0.2$, $T_h = 300$ K and $T_i = 0.05$ K. (c) Blue solid, red dashed, and black dot-dashed curves are for $\alpha_i = 0.05, 0.1, 0.2$, respectively. $T_h = 300$ K and $T_i = 0.1$ K. (d) Blue solid, red dashed, and black dot-dashed curves are for $T_i = 0.1, 0.15, 0.2$ K, respectively. $T_h = 300$ K and $\alpha_i = 0.2$.

here P denotes the principal value. The bath modes closer to the resonance frequency ω_q^r are more strongly coupled to the system.

We shall discuss the entanglement generation in two different situations, depending upon the frequencies of the resonators.

A. Non-degenerate resonators

First we discuss the case in which difference between the frequencies of resonators is large. If we consider the resonance frequency of the hot bath filter $\omega_h^r = \omega_a - \sum_i \omega_i$ and of the cold bath filter $\omega_c^r = \omega_a$ in Eq. (18) (shown in Fig. 1(b)), this choice leads to Liouville super-operators of the hot and cold bath of the form

$$\begin{aligned} \tilde{\mathcal{L}}_c^d \tilde{\rho} &= \tilde{f}_c(\omega_a) \{ D[\tilde{a}] + \alpha^3 \sum_i D[\tilde{a} \tilde{b}_i^\dagger \tilde{b}_i] \} \\ &\quad + \tilde{f}_c(-\omega_a) \{ D[\tilde{a}^\dagger] + \sum_i \alpha^3 D[\tilde{a}^\dagger \tilde{b}_i^\dagger \tilde{b}_i] \}, \\ \tilde{\mathcal{L}}_h^d \tilde{\rho} &= \alpha^3 \{ \tilde{f}_h(\omega_-) D[\tilde{a} \tilde{b}_1^\dagger \tilde{b}_2^\dagger] + \tilde{f}_h(-\omega_-) D[\tilde{a}^\dagger \tilde{b}_1 \tilde{b}_2] \}, \\ \tilde{\mathcal{L}}_i \tilde{\rho} &= f_i(\omega_i) D[\tilde{b}_i] + f_i(-\omega_i) D[\tilde{b}_i^\dagger], \end{aligned} \quad (20)$$

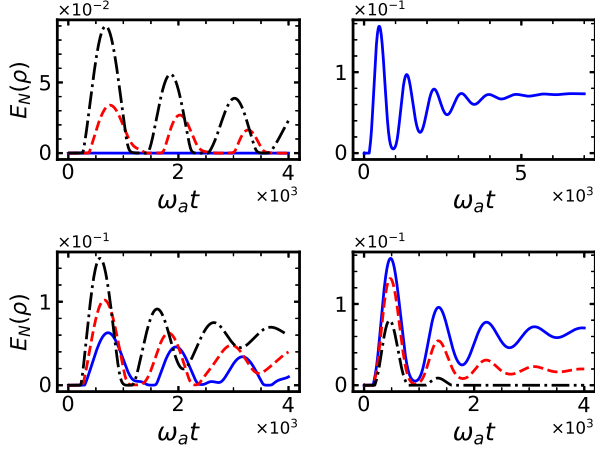


FIG. 4. Entanglement quantification of resonators with same frequencies. Logarithmic negativity $E_N(\rho)$ as a function of scaled time $\omega_a t$. The results are obtained by the numerical integration of Eq. (21) and then using the inverse transformation [Eq. (6)] to get $\hat{\rho}$ in the *local* basis. Finally, $E_N(\rho)$ is computed numerically using Eq. (17). Initial state of the system is considered a pure separable state of the subsystems, $\hat{\rho}(0) = \hat{\rho}_a \otimes \hat{\rho}_1 \otimes \hat{\rho}_2 = |g_a\rangle \langle g_a| \otimes |0_1\rangle \langle 0_1| \otimes |0_2\rangle \langle 0_2|$, here $|g_a\rangle$ represents the ground state of the TLS. Parameters: $\omega_a = 2\pi \times 10$ GHz, $\omega_1 = \omega_2 = 2\pi \times 5$ MHz, $\gamma_h = \gamma_c = 2\pi \times 500$ KHz, $\gamma_i = 2\pi \times 100$ Hz, and $T_c = 65$ mK. All the parameters are scaled with ω_a in the numerical results. (a) Blue solid, red dashed, and black dot-dashed curves are for $T_h = 1, 70, 300$ K, respectively. Here, $T_i = 0.1$ K and $\alpha_i = 0.1$. (b) Long time entanglement $E_N(\rho)$ for $\alpha_i = 0.2$, $T_h = 300$ K and $T_i = 0.05$ K. (c) Blue solid, red dashed, and black dot-dashed curves are for $\alpha_i = 0.05, 0.1, 0.2$, respectively. $T_h = 300$ K and $T_i = 0.1$. (d) Blue solid, red dashed, and black dot-dashed curves are for $T_i = 0.1, 0.15, 0.2$ K, respectively. $T_h = 300$ K and $\alpha_i = 0.2$. All the curves show an almost periodic behavior of $E_N(\rho)$ with a period of $T \approx 4\pi/\sum_i \omega_i$.

with $\omega_- = \omega_a - \sum_i \omega_i$ and $\tilde{\mathcal{L}}_i$ remains unchanged. For $T_h \gg T_i > T_c$ and $\gamma_i \bar{n}_i \ll \alpha^3 \tilde{f}_h(\omega_-)$, D_{ent} is the dominant source of dissipation in the system. This leads to considerable degree of entanglement between the resonators R_i . In rest of the work, resonators R_i are considered in an initial separable state of their ground states. This initial state could be achieved without the need for external control drive in our scheme. Simultaneous ground state cooling of the resonators can be achieved in the limit $T_h \gg T_i > T_c$ by tuning the resonance frequency of the hot bath filter at the first lower sideband [see Eq. (18)] [54]. Then one switch the resonance frequency to lower second order sideband, soon after resonators cool to their ground states.

Time dependence of logarithmic negativity $E_N(\hat{\rho})$, in case of TLS- R_i system is shown in Fig. 3. For $T_h \sim T_i > T_c$, there is no entanglement between resonators R_i because $\tilde{\mathcal{L}}_i$ dominates the dissipation dynamics in this limit. In case of $T_h \gg T_i > T_c$, entanglement between the resonators emerges and it increases with the higher values of T_h , shown in Fig. 3(a). Entanglement $E_N(\hat{\rho})$ between the resonators in the long-time limit is shown in Fig. 3(b). Compared with

Fig. 2 results, there is no periodic behavior of entanglement in Fig. 3. This is because in Fig. 3, we consider non-degenerate resonators R_i , which gives non-synchronized dynamics of the mean number of excitations $\hat{n}_i = \langle \hat{b}_i^\dagger \hat{b}_i \rangle$. As shown in Fig. 2, \hat{n}_i governs the dynamics of $E_N(\hat{\rho})$, hence, non-synchronized dynamics of \hat{n}_i suggests the absence of periodicity in $E_N(\hat{\rho})$. The increase in entanglement with the increase in coupling strength g_i between TLS and resonators is presented in Fig. 3(c). We check the robustness of entanglement between the resonators against thermal vibrations in Fig. 3(d).

These results show that the early time entanglement is reasonably robust against resonators environment temperature provided sufficiently large α and $T_h \gg T_i > T_c$. However, for large bath temperatures $T_i \gg \omega_a$, entanglement shows damped oscillations and vanishes in the long-time limit. We note that for higher bath temperatures T_i , larger values of α and very high hot bath temperature T_h are required to generate long-time entanglement between the resonators. This is because $D[\tilde{a}^\dagger \tilde{b}_1 \tilde{b}_2]$ is responsible for both cooling and creating entanglement. For $T_i \gg \omega_a$, stronger coupling strength g_i and very high-temperature T_h are required to cool the resonators. The use of a third common bath to enhance the entanglement by cooling the system is consistent with previously reported results [81]. In this scheme, entanglement enhancement is shown by cooling a pair of qubits via a shared bath. Alternatively, the hot bath can be replaced by a squeezed thermal bath or reservoir with a negative temperature to enhance the cooling and entanglement between resonators [36].

B. Degenerate resonators

For the case of degenerate resonators $\omega_1 = \omega_2 = \Omega$, if we select the resonance frequency of the hot bath $\omega_h^r = \omega_a - 2\Omega$, and of the cold bath $\omega_c^r = \omega_a$ in Eq. (18), the master equation (9) reduces to

$$\begin{aligned} \tilde{\mathcal{L}}_c^s \tilde{\rho} &= \tilde{\mathcal{L}}_c^d \tilde{\rho} + \alpha^3 \tilde{f}_c(\omega_a) \{D[\tilde{a} \tilde{b}_1^\dagger \tilde{b}_2] + D[\tilde{a} \tilde{b}_1 \tilde{b}_2^\dagger]\} \\ &\quad + \alpha^3 \tilde{f}_c(-\omega_a) \{D[\tilde{a}^\dagger \tilde{b}_1 \tilde{b}_2] + D[\tilde{a}^\dagger \tilde{b}_1^\dagger \tilde{b}_2]\}, \\ \tilde{\mathcal{L}}_h^s \tilde{\rho} &= \tilde{\mathcal{L}}_h^d \tilde{\rho} + \alpha^3 \{\tilde{f}_h(\omega_a - 2\Omega) \sum_i D[\tilde{a} \tilde{b}_i^{\dagger 2}] \\ &\quad + \tilde{f}_h(-\omega_a + 2\Omega) \sum_i D[\tilde{a}^\dagger \tilde{b}_i^2]\}, \\ \tilde{\mathcal{L}}_i \tilde{\rho} &= f_i(\Omega) D[\tilde{b}_i] + f_i(-\Omega) D[\tilde{b}_i^\dagger]. \end{aligned} \quad (21)$$

There are additional terms in Eq. (21) compared with Eq. (20). We consider $T_c \ll 1$ K in our results, hence, the impact of additional terms of $\tilde{\mathcal{L}}_c^s \tilde{\rho}$ on entanglement generation is not significant. Contrary, the second and third terms of $\tilde{\mathcal{L}}_c^s \tilde{\rho}$ dissipation rates depends on T_h , consequently, have non-negligible negative effect on the entanglement. The results in Fig. 4 confirms the decrease in the entanglement for the degenerate resonators due to the presence of additional terms in Eq. (21). In Fig. 4, boAccordingly, the cooling of the mechanical resonators is accompanied by entanglement generation (). This analysis is confirmed by the numerical results presented in Fig. 5, which show that the cooling and entanglement co-occur in our scheme. For the entanglement generation, the

ground state of the resonators is an optimal choice. Fig. 5 shows that the thermal state with sufficiently low excitations n_i can also be considered. The resonators are identical, which leads to synchronized dynamics of the mean excitations $\langle \tilde{b}_i^\dagger \tilde{b}_i \rangle$. In addition, both populations and entanglement show periodic oscillations with a period of $T = 2\pi/\Omega$. Note that the early time entanglement behavior is monotonic as a function of the hot bath temperature, as shown in Fig. 4(a). This is in contrast to previous works [25, 35], where entanglement increases to a maximum value for the optimal value of driving heat bath temperature, and then decreases to zero for higher temperatures.

Our proposal can be experimentally realized using an electro-mechanical system [57] or circuit QED setup [49]. The system consists of a superconducting microwave resonator (SR), or a qubit of frequency ω_a , which is simultaneously coupled to two micromechanical resonators [57], or microwave resonators [49, 58] of frequency ω_i . Spectrally filtered hot and cold baths at temperatures T_h and T_c drive the SR, respectively. In addition, two microwave resonators designed at frequencies $\omega_- = \omega_a - 2\sum_i \omega_i$, and ω_a couple to the SR for the realization of the hot and cold baths spectrum filtering, respectively. For the implementation of the thermal baths, each of these microwave resonators is coupled to a copper thin-film resistor [82]. The spectral density of the bath provided by these resistors can be modeled by Ohmic spectral density [83]. In the bath spectrum filtering, it is possible to map the microwave resonators (coupled to the SR or qubit) and the baths to a structured environment of non-interacting harmonic oscillators with an effective spectral density given by Lorentzian function [84]. The judicious choice of the microwave resonator frequencies completely suppresses or weakens the undesired bath-induced transitions.

V. CONCLUSIONS

We proposed and analyzed an autonomous quantum thermal machine to generate transient and steady-state entanglement of two uncoupled macroscopic mechanical resonators. Unlike previous proposals on reservoir engineering, our quantum entanglement engine does not rely on external control or work input to generate entanglement between uncoupled macroscopic mechanical resonators. Entanglement between two uncoupled resonators is created by coupling them to a common incoherently driven two-level system or a harmonic oscillator. We proposed bath spectrum filtering to engineer desirable incoherent interaction with the thermal baths to create entanglement, which is a critical step in our scheme. Our numerical results showed a significantly large amount of entanglement established between the resonators in the absence of thermal equilibrium and even in the presence of the local dissipation of the resonators. In addition, the amount of early time entanglement showed a monotonic increase with the increase in a temperature gradient. To the best of our knowledge, there are no reported results of steady-state entanglement generation between uncoupled mechanical resonators using temperature gradient. If we consider circuit QED implementation

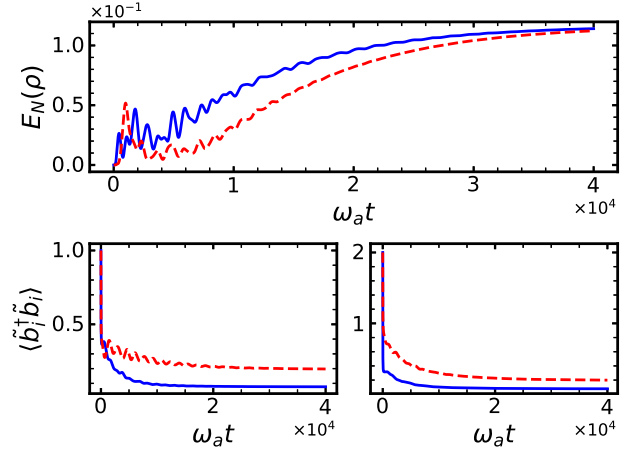


FIG. 5. (a) Entanglement quantification $E_N(\rho)$ of the resonators with different initial thermal states as a function of scaled time $\omega_a t$. The solid and dashed lines represent the initial thermal state of the resonators with the mean excitation $\bar{n}_i = 1, 2$, respectively. The results are obtained by the numerical integration of Eq. (20) and then using the inverse transformation [Eq. (6)] to get $\hat{\rho}$ in the *local* basis. Finally, $E_N(\rho)$ is computed numerically using Eq. (17). (b), and (c) show the mean phonon number $\langle \tilde{b}_i^\dagger \tilde{b}_i \rangle$ for initial mean excitation $\bar{n}_i = 1, 2$, as a function of scaled time $\omega_a t$, respectively. The solid and dashed lines are for the resonators R_1 and R_2 , respectively. Parameters: $\omega_a = 2\pi \times 10$ GHz, $\omega_1 = 2\omega_2 = 2\pi \times 5$ MHz, $\gamma_h = \gamma_c = 2\pi \times 500$ KHz, $\gamma_i = 2\pi \times 100$ Hz, $\alpha_i = 0.2$, $T_h = 300$ K, $T_c = 65$ mK and $T_i = 0.05$ K. All the parameters are scaled with ω_a in the numerical results.

of our scheme, then entanglement generation may be compared with Ref. [25] in which entanglement between two optical cavities is investigated in a similar setting. In our system, entanglement is almost two orders of magnitude larger than reported in Ref. [25].

The periodic oscillations in the entanglement are reported for the resonators of the same frequency. For the non-degenerate case, the periodicity breaks down due to the non-synchronized dynamics of the resonators. For the experimental realizations, several physical systems are conceivable such as optomechanical system [48], circuit QED [49, 59], and electro-mechanical systems [64]. Our results suggest that bath spectrum filtering can provide an alternative to typical reservoir engineering schemes to create non-classical states. Bath spectrum filtering does not require external control for the desirable engineering of the dissipative dynamics. Hence, it can be a promising route for creating exotic quantum states, useful for metrology or quantum computation [1].

ACKNOWLEDGMENTS

We thank André Xuereb for the fruitful discussions.

Appendix A: Simultaneous entanglement and cooling of the resonators

In a typical optomechanical system, simultaneous entanglement and cooling of the resonators are not possible. The reason is that cooling of the resonators requires beam splitter interaction, and entanglement generation between the resonators is possible with two-mode squeezing interaction. Depending on the input laser drive frequency choice, one of these two interactions can be made resonant. Accordingly, entanglement and cooling occur in two separate sets of system parameters [48]. On the contrary, in our scheme, both entanglement and cooling of the resonators can co-occur. This is one of the key features of our scheme, and to the best of our knowledge, it is not reported in the bosonic out-of-equilibrium entanglement generation schemes too.

To investigate the entanglement and cooling of the resonators, after tracing the ancilla system A, Eq. (20) is given by

$$\begin{aligned} \frac{d\tilde{\rho}}{dt} = & \sum_i (\gamma_{i,\downarrow} D[\tilde{b}_i] + \gamma_{i,\uparrow} D[\tilde{b}_i^\dagger] + \gamma_d D[\tilde{b}_1^\dagger \tilde{b}_2]) \\ & + \Gamma_\downarrow D[\tilde{b}_1 \tilde{b}_2] + \Gamma_\uparrow D[\tilde{b}_1^\dagger \tilde{b}_2^\dagger], \end{aligned} \quad (\text{A1})$$

here, we define

$$\begin{aligned} \gamma_{i,\downarrow} &= f_i(\omega_i), \quad \gamma_{i,\uparrow} = f_i(-\omega_i), \\ \Gamma_\downarrow &= \alpha^3 \tilde{f}(-\omega_-) \langle \tilde{n}_a + 1 \rangle, \\ \Gamma_\uparrow &= \alpha^3 \tilde{f}(\omega_-) \langle \tilde{n}_a \rangle, \\ \gamma_d &= \alpha^3 (\tilde{f}(\omega_a) \langle \tilde{n}_a \rangle + \tilde{f}(-\omega_a) \langle \tilde{n}_a + 1 \rangle). \end{aligned} \quad (\text{A2})$$

For sufficiently low excitations \tilde{n}_i in the resonators and $T_h \gg T_i > T_c$, the simultaneous cooling rate Γ_\downarrow becomes larger than the simultaneous Γ_\uparrow and the individual heating rates $\gamma_{i,\uparrow}$ of the resonators [54]. Accordingly, the cooling of the mechanical resonators is accompanied by entanglement generation (see Sec. IV A). This analysis is confirmed by the numerical results presented in Fig. 5, which show that the cooling and entanglement co-occur in our scheme. Due to the different frequencies of the resonators, cooling rates are different [54, 85]. For the optimal performance of our scheme, the resonators should be considered in their ground states. However, this is not a requirement, as Fig. 5 shows that the thermal state with sufficiently low excitations \tilde{n}_i can also lead to entanglement between the resonators.

-
- [1] Antonio Acín, Immanuel Bloch, Harry Buhrman, Tommaso Calarco, Christopher Eichler, Jens Eisert, Daniel Esteve, Nicolas Gisin, Steffen J Glaser, Fedor Jelezko, Stefan Kuhr, Maciej Lewenstein, Max F Riedel, Piet O Schmidt, Rob Thew, Andreas Wallraff, Ian Walmsley, and Frank K Wilhelm, “The quantum technologies roadmap: a european community view,” *New J. Phys.* **20**, 080201 (2018).
 - [2] Daniel Burgarth and Vittorio Giovannetti, “Mediated homogenization,” *Phys. Rev. A* **76**, 062307 (2007).
 - [3] B. Kraus, H. P. Büchler, S. Diehl, A. Kantian, A. Micheli, and P. Zoller, “Preparation of entangled states by quantum markov processes,” *Phys. Rev. A* **78**, 042307 (2008).
 - [4] S. Diehl, A. Micheli, A. Kantian, B. Kraus, H. P. Büchler, and P. Zoller, “Quantum states and phases in driven open quantum systems with cold atoms,” *Nat. Phys.* **4**, 878–883 (2008).
 - [5] Frank Verstraete, Michael M. Wolf, and J. Ignacio Cirac, “Quantum computation and quantum-state engineering driven by dissipation,” *Nat. Phys.* **5**, 633–636 (2009).
 - [6] Susanne Pielawa, Giovanna Morigi, David Vitali, and Luiz Davidovich, “Generation of einstein-podolsky-rosen-entangled radiation through an atomic reservoir,” *Phys. Rev. Lett.* **98**, 240401 (2007).
 - [7] Susanne Pielawa, Luiz Davidovich, David Vitali, and Giovanna Morigi, “Engineering atomic quantum reservoirs for photons,” *Phys. Rev. A* **81**, 043802 (2010).
 - [8] Jianming Cai, Sandu Popescu, and Hans J. Briegel, “Dynamic entanglement in oscillating molecules and potential biological implications,” *Phys. Rev. E* **82**, 021921 (2010).
 - [9] M. J. Kastoryano, F. Reiter, and A. S. Sørensen, “Dissipative preparation of entanglement in optical cavities,” *Phys. Rev. Lett.* **106**, 090502 (2011).
 - [10] Christian Arenz, Cecilia Cormick, David Vitali, and Giovanna Morigi, “Generation of two-mode entangled states by quantum reservoir engineering,” *J. Phys. B: At. Mol. Opt. Phys.* **46**, 224001 (2013).
 - [11] Stefan Walter, Jan Carl Budich, Jens Eisert, and Björn Trauzettel, “Entanglement of nanoelectromechanical oscillators by cooper-pair tunneling,” *Phys. Rev. B* **88**, 035441 (2013).
 - [12] Florentin Reiter, L. Tornberg, Göran Johansson, and Anders S. Sørensen, “Steady-state entanglement of two superconducting qubits engineered by dissipation,” *Phys. Rev. A* **88**, 032317 (2013).
 - [13] M. J. A. Schuetz, E. M. Kessler, L. M. K. Vandersypen, J. I. Cirac, and G. Giedke, “Steady-state entanglement in the nuclear spin dynamics of a double quantum dot,” *Phys. Rev. Lett.* **111**, 246802 (2013).
 - [14] Hanna Krauter, Christine A. Muschik, Kasper Jensen, Wojciech Wasilewski, Jonas M. Petersen, J. Ignacio Cirac, and Eugene S. Polzik, “Entanglement generated by dissipation and steady state entanglement of two macroscopic objects,” *Phys. Rev. Lett.* **107**, 080503 (2011).
 - [15] Julio T. Barreiro, Markus Müller, Philipp Schindler, Daniel Nigg, Thomas Monz, Michael Chwalla, Markus Hennrich, Christian F. Roos, Peter Zoller, and Rainer Blatt, “An open-system quantum simulator with trapped ions,” *Nature* **470**, 486–491 (2011).
 - [16] Y. Lin, J. P. Gaebler, F. Reiter, T. R. Tan, R. Bowler, A. S. Sørensen, D. Leibfried, and D. J. Wineland, “Dissipative pro-

- duction of a maximally entangled steady state of two quantum bits,” *Nature* **504**, 415–418 (2013).
- [17] S. Shankar, M. Hatridge, Z. Leghtas, K. M. Sliwa, A. Narla, U. Vool, S. M. Girvin, L. Frunzio, M. Mirrahimi, and M. H. Devoret, “Autonomously stabilized entanglement between two superconducting quantum bits,” *Nature* **504**, 419–422 (2013).
- [18] Ying-Dan Wang and Aashish A. Clerk, “Reservoir-engineered entanglement in optomechanical systems,” *Phys. Rev. Lett.* **110**, 253601 (2013).
- [19] M. J. Woolley and A. A. Clerk, “Two-mode squeezed states in cavity optomechanics via engineering of a single reservoir,” *Phys. Rev. A* **89**, 063805 (2014).
- [20] Jie-Qiao Liao, Qin-Qin Wu, and Franco Nori, “Entangling two macroscopic mechanical mirrors in a two-cavity optomechanical system,” *Phys. Rev. A* **89**, 014302 (2014).
- [21] J Li, I Moaddel Haghighi, N Malossi, S Zippilli, and D Vitali, “Generation and detection of large and robust entanglement between two different mechanical resonators in cavity optomechanics,” *New J. Phys.* **17**, 103037 (2015).
- [22] M. C. Arnesen, S. Bose, and V. Vedral, “Natural thermal and magnetic entanglement in the 1d heisenberg model,” *Phys. Rev. Lett.* **87**, 017901 (2001).
- [23] D. Gunlycke, V. M. Kendon, V. Vedral, and S. Bose, “Thermal concurrence mixing in a one-dimensional ising model,” *Phys. Rev. A* **64**, 042302 (2001).
- [24] M. B. Plenio, S. F. Huelga, A. Beige, and P. L. Knight, “Cavity-loss-induced generation of entangled atoms,” *Phys. Rev. A* **59**, 2468–2475 (1999).
- [25] M. B. Plenio and S. F. Huelga, “Entangled light from white noise,” *Phys. Rev. Lett.* **88**, 197901 (2002).
- [26] S. Schneider and G. J. Milburn, “Entanglement in the steady state of a collective-angular-momentum (dicke) model,” *Phys. Rev. A* **65**, 042107 (2002).
- [27] M. S. Kim, Jinhyoung Lee, D. Ahn, and P. L. Knight, “Entanglement induced by a single-mode heat environment,” *Phys. Rev. A* **65**, 040101 (2002).
- [28] Daniel Braun, “Creation of entanglement by interaction with a common heat bath,” *Phys. Rev. Lett.* **89**, 277901 (2002).
- [29] Fabio Benatti, Roberto Floreanini, and Marco Piani, “Environment induced entanglement in markovian dissipative dynamics,” *Phys. Rev. Lett.* **91**, 070402 (2003).
- [30] L. Hartmann, W. Dür, and H.-J. Briegel, “Steady-state entanglement in open and noisy quantum systems,” *Phys. Rev. A* **74**, 052304 (2006).
- [31] Luis Quiroga, Ferney J. Rodríguez, María E. Ramírez, and Roberto París, “Nonequilibrium thermal entanglement,” *Phys. Rev. A* **75**, 032308 (2007).
- [32] Ilya Sinaysky, Francesco Petruccione, and Daniel Burgarth, “Dynamics of nonequilibrium thermal entanglement,” *Phys. Rev. A* **78**, 062301 (2008).
- [33] Lian-Ao Wu and Dvira Segal, “Quantum effects in thermal conduction: Nonequilibrium quantum discord and entanglement,” *Phys. Rev. A* **84**, 012319 (2011).
- [34] Bruno Bellomo and Mauro Antezza, “Creation and protection of entanglement in systems out of thermal equilibrium,” *New J. Phys.* **15**, 113052 (2013).
- [35] Jonatan Bohr Brask, Géraldine Haack, Nicolas Brunner, and Marcus Huber, “Autonomous quantum thermal machine for generating steady-state entanglement,” *New J. Physics* **17**, 113029 (2015).
- [36] F. Tacchino, A. Auffèves, M. F. Santos, and D. Gerace, “Steady state entanglement beyond thermal limits,” *Phys. Rev. Lett.* **120**, 063604 (2018).
- [37] Karen V Hovhannisyan and Alberto Imparato, “Quantum current in dissipative systems,” *New J. Physics* **21**, 052001 (2019).
- [38] Zhihai Wang, Wei Wu, and Jin Wang, “Steady-state entanglement and coherence of two coupled qubits in equilibrium and nonequilibrium environments,” *Phys. Rev. A* **99**, 042320 (2019).
- [39] Shishir Khandelwal, Nicolas Palazzo, Nicolas Brunner, and Géraldine Haack, “Critical heat current for operating an entanglement engine,” *New J. Physics* **22**, 073039 (2020).
- [40] Armin Tavakoli, Géraldine Haack, Nicolas Brunner, and Jonatan Bohr Brask, “Autonomous multipartite entanglement engines,” *Phys. Rev. A* **101**, 012315 (2020).
- [41] Daniel Heineken, Konstantin Beyer, Kimmo Luoma, and Walter T. Strunz, “Quantum-memory-enhanced dissipative entanglement creation in nonequilibrium steady states,” *Phys. Rev. A* **104**, 052426 (2021).
- [42] Kun Zhang and Jin Wang, “Entanglement versus bell nonlocality of quantum nonequilibrium steady states,” *Quant. Inf. Process.* **20**, 147 (2021).
- [43] Shishir Khandelwal, Nicolas Brunner, and Géraldine Haack, “Signatures of liouvillian exceptional points in a quantum thermal machine,” *PRX Quantum* **2**, 040346 (2021).
- [44] Jonatan Bohr Brask, Fabien Clivaz, Géraldine Haack, and Armin Tavakoli, “Operational nonclassicality in minimal autonomous thermal machines,” *Quantum* **6**, 672 (2022).
- [45] Pradip Laha, Lukáš Slodička, Darren W. Moore, and Radim Filip, “Thermally induced entanglement of atomic oscillators,” *Opt. Express* **30**, 8814–8828 (2022).
- [46] Armin Tavakoli, Géraldine Haack, Marcus Huber, Nicolas Brunner, and Jonatan Bohr Brask, “Heralded generation of maximal entanglement in any dimension via incoherent coupling to thermal baths,” *Quantum* **2**, 73 (2018).
- [47] Ze-Liang Xiang, Sahel Ashhab, J. Q. You, and Franco Nori, “Hybrid quantum circuits: Superconducting circuits interacting with other quantum systems,” *Rev. Mod. Phys.* **85**, 623–653 (2013).
- [48] Markus Aspelmeyer, Tobias J. Kippenberg, and Florian Marquardt, “Cavity optomechanics,” *Rev. Mod. Phys.* **86**, 1391–1452 (2014).
- [49] C. Eichler and J. R. Petta, “Realizing a circuit analog of an optomechanical system with longitudinally coupled superconducting resonators,” *Phys. Rev. Lett.* **120**, 227702 (2018).
- [50] A.G. Kofman, G. Kurizki, and B. Sherman, “Spontaneous and induced atomic decay in photonic band structures,” *J. Mod. Opt.* **41**, 353–384 (1994).
- [51] A. Ghosh, C. L. Latune, L. Davidovich, and G. Kurizki, “Catalysis of heat-to-work conversion in quantum machines,” *Proc. Natl. Acad. Sci.* **114**, 12156–12161 (2017).
- [52] M. Tahir Naseem, A. Misra, and Özgür E. Müstecaplıoğlu, “Two-body quantum absorption refrigerators with optomechanical-like interactions,” *Quantum Sci. Technol.* **5**, 035006 (2020).
- [53] M. Tahir Naseem, A. Misra, Özgür E. Müstecaplıoğlu, and G. Kurizki, “Minimal quantum heat manager boosted by bath spectral filtering,” *Phys. Rev. Research* **2**, 033285 (2020).
- [54] M. Tahir Naseem and Özgür E. Müstecaplıoğlu, “Ground-state cooling of mechanical resonators by quantum reservoir engineering,” *Commun. Phys.* **4**, 95 (2021).
- [55] M. Tahir Naseem and Özgür E. Müstecaplıoğlu, “Antibunching via cooling by heating,” *Phys. Rev. A* **105**, 012201 (2022).
- [56] P. Rabl, “Photon blockade effect in optomechanical systems,” *Phys. Rev. Lett.* **107**, 063601 (2011).
- [57] Francesco Massel, Sung Un Cho, Juha-Matti Pirkkalainen, Pertti J. Hakonen, Tero T. Heikkilä, and Mika A. Sillanpää, “Multimode circuit optomechanics near the quantum limit,”

- Nat. Commun. **3**, 987 (2012).
- [58] Nicolas Didier, Jérôme Bourassa, and Alexandre Blais, “Fast quantum nondemolition readout by parametric modulation of longitudinal qubit-oscillator interaction,” *Phys. Rev. Lett.* **115**, 203601 (2015).
- [59] D. Bothner, I. C. Rodrigues, and G. A. Steele, “Photon-pressure strong coupling between two superconducting circuits,” *Nat. Phys.* **17**, 85–91 (2021).
- [60] I. Wilson-Rae, P. Zoller, and A. Imamoglu, “Laser cooling of a nanomechanical resonator mode to its quantum ground state,” *Phys. Rev. Lett.* **92**, 075507 (2004).
- [61] P. Zhang, Y. D. Wang, and C. P. Sun, “Cooling mechanism for a nanomechanical resonator by periodic coupling to a cooper pair box,” *Phys. Rev. Lett.* **95**, 097204 (2005).
- [62] Ying-Dan Wang, Yong Li, Fei Xue, C. Bruder, and K. Semba, “Cooling a micromechanical resonator by quantum back-action from a noisy qubit,” *Phys. Rev. B* **80**, 144508 (2009).
- [63] P. Rabl, P. Cappellaro, M. V. Gurudev Dutt, L. Jiang, J. R. Maze, and M. D. Lukin, “Strong magnetic coupling between an electronic spin qubit and a mechanical resonator,” *Phys. Rev. B* **79**, 041302 (2009).
- [64] M. D. LaHaye, J. Suh, P. M. Echternach, K. C. Schwab, and M. L. Roukes, “Nanomechanical measurements of a superconducting qubit,” *Nature* **459**, 960–964 (2009).
- [65] Jalil Khatibi Moqadam, Renato Portugal, and Marcos Cesar de Oliveira, “Quantum walks on a circle with optomechanical systems,” *Quant. Info. Proc.* **14**, 3595–3611 (2015).
- [66] M. Kolář, D. Gelbwaser-Klimovsky, R. Alicki, and G. Kurizki, “Quantum bath refrigeration towards absolute zero: Challenging the unattainability principle,” *Phys. Rev. Lett.* **109**, 090601 (2012).
- [67] I. G. Lang and Yu. A. Firsov, “Kinetic Theory of Semiconductors with Low Mobility,” *Soviet Journal of Experimental and Theoretical Physics* **16**, 1301 (1963).
- [68] Susanne Richer and David DiVincenzo, “Circuit design implementing longitudinal coupling: A scalable scheme for superconducting qubits,” *Phys. Rev. B* **93**, 134501 (2016).
- [69] M. Tahir Naseem, André Xuereb, and Özgür E. Müstecaplıoğlu, “Thermodynamic consistency of the optomechanical master equation,” *Phys. Rev. A* **98**, 052123 (2018).
- [70] D. Gelbwaser-Klimovsky and G. Kurizki, “Heat-machine control by quantum-state preparation: From quantum engines to refrigerators,” *Phys. Rev. E* **90**, 022102 (2014).
- [71] J. D. Teufel, T. Donner, Dale Li, J. W. Harlow, M. S. Allman, K. Cicak, A. J. Sirois, J. D. Whittaker, K. W. Lehnert, and R. W. Simmonds, “Sideband cooling of micromechanical motion to the quantum ground state,” *Nature* **475**, 359–363 (2011).
- [72] A. Nunnenkamp, K. Børkje, and S. M. Girvin, “Cooling in the single-photon strong-coupling regime of cavity optomechanics,” *Phys. Rev. A* **85**, 051803 (2012).
- [73] M. B. Plenio, “Logarithmic negativity: A full entanglement monotone that is not convex,” *Phys. Rev. Lett.* **95**, 090503 (2005).
- [74] Martin B. Plenio and Shashank Virmani, “An introduction to entanglement measures,” *Quantum Inf. Comput.* **7**, 1–51 (2007).
- [75] Ryszard Horodecki, Paweł Horodecki, Michał Horodecki, and Karol Horodecki, “Quantum entanglement,” *Rev. Mod. Phys.* **81**, 865–942 (2009).
- [76] G. Vidal and R. F. Werner, “Computable measure of entanglement,” *Phys. Rev. A* **65**, 032314 (2002).
- [77] B. P. Lanyon, C. Maier, M. Holzäpfel, T. Baumgratz, C. Hempel, P. Jurcevic, I. Dhand, A. S. Buyskikh, A. J. Daley, M. Cramer, M. B. Plenio, R. Blatt, and C. F. Roos, “Efficient tomography of a quantum many-body system,” *Nat. Phys.* **13**, 1158–1162 (2017).
- [78] Andreas Elben, Richard Kueng, Hsin-Yuan (Robert) Huang, Rick van Bijnen, Christian Kokail, Marcello Dalmonte, Pasquale Calabrese, Barbara Kraus, John Preskill, Peter Zoller, and Benoît Vermersch, “Mixed-state entanglement from local randomized measurements,” *Phys. Rev. Lett.* **125**, 200501 (2020).
- [79] Aurora Voje, Andreas Isacsson, and Alexander Croy, “Nonlinear-dissipation-induced entanglement of coupled nonlinear oscillators,” *Phys. Rev. A* **88**, 022309 (2013).
- [80] David Gelbwaser-Klimovsky, Wolfgang Niedenzu, and Gershon Kurizki, “Chapter twelve - thermodynamics of quantum systems under dynamical control,” (Academic Press, 2015) pp. 329–407.
- [81] Zhong-Xiao Man, Armin Tavakoli, Jonatan Bohr Brask, and Yun-Jie Xia, “Improving autonomous thermal entanglement generation using a common reservoir,” *Phys. Scr.* **94**, 075101 (2019).
- [82] Jorden Senior, Azat Gubaydullin, Bayan Karimi, Joonas T. Peltonen, Joachim Ankerhold, and Jukka P. Pekola, “Heat rectification via a superconducting artificial atom,” *Commun. Phys.* **3**, 40 (2020).
- [83] David Zueco, Peter Hänggi, and Sigmund Kohler, “Landau–Zener tunnelling in dissipative circuit QED,” *New J. Phys.* **10**, 115012 (2008).
- [84] Mariano Bonifacio, Daniel Domínguez, and María José Sánchez, “Landau-zener-stückelberg interferometry in dissipative circuit quantum electrodynamics,” *Phys. Rev. B* **101**, 245415 (2020).
- [85] Claudiu Genes, David Vitali, and Paolo Tombesi, “Simultaneous cooling and entanglement of mechanical modes of a micromirror in an optical cavity,” *New J. Phys.* **10**, 095009 (2008).